BNL-219835-2020-JAAM

A bilayer anion-exchange membrane with low borohydride crossover and improved fuel efficiency for direct borohdyride fuel cell

X. Li, Y. S. Chu

To be published in "ACS APPLIED MATERIALS & INTERFACES"

June 2020

Photon Sciences

Brookhaven National Laboratory

U.S. Department of Energy

USDOE Office of Science (SC), Basic Energy Sciences (BES) (SC-22)

DISCLAIMER

A bilayer anion-exchange membrane with low borohydride crossover and improved fuel efficiency for direct borohdyride fuel cell

Xingxing Li†, Haodong Chen†, Wen Chu‡, Haiying Qin†, Wen Zhang†, Hualiang Ni†, Hongzhong Chi†, Yan He$, Yong S. Chu%, Jianan Hu&, Jiabin Liu‡*

† College of Materials and Environmental Engineering, Hangzhou Dianzi University, Hangzhou 310018, P. R. China.

‡ School of Materials Science and Engineering, Zhejiang University, Hangzhou 310027, P. R. China.

$ Shanghai Synchrotron Radiation Facility, Shanghai Institute of Applied Physics, Chinese Academy of Sciences, Shanghai, 201800, P. R. China.

% National Synchrotron Light Source II, Brookhaven National Laboratory, Upton, New York 11973, USA.

& College of Light Industry and Food Engineering, Nanjing forestry University, Nanjing 210037, P. R. China.

KEYWORDS: Direct borohydride fuel cell; Anion-exchange membrane; Bilayer membrane; Crossover; Fuel efficiency

ABSTRACT: The development of membranes with low fuel crossover and high fuel efficiency is a key issue for direct borohydride fuel cells (DBFC). In previous work, we produced a polyvinyl alcohol (PVA) - anion exchange resin (AER) membrane with low fuel crossover and low fuel efficiency by introducing Co ions. In this work, a bilayer membrane was designed to improve fuel efficiency and cell performance. The bilayer membrane was prepared by casting a PVA-AER wet gel onto the partially desiccated Co-PVA-AER gel. The bilayer membrane showed a borohydride permeability of 1.34×10^{-6} $cm^2 \cdot s^{-1}$, which was even lower than that of the Co-PVA-AER membrane (1.98×10^{-6} $cm^2 \cdot s^{-1}$) and the PVA-AER membrane (2.80×10^{-6} $cm^2 \cdot s^{-1}$). The DBFC using the bilayer membrane exhibited higher fuel efficiency (37.4%) and output power (1.73 Wh) than the DBFCs using the Co-PVA-AER membrane (33.3%, 1.27 Wh) and the PVA-AER membrane (34.3%, 1.2 Wh). Furthermore, the DBFC using the bilayer membrane achieved a peak power density of 327 $mW \cdot cm^{-2}$, which was 2.14 times of that of the DBFC using the PVA-AER membrane (153 $mW \cdot cm^{-2}$). The drastic improvement benefited from the bilayer design, which introduced an interphase to suppress fuel crossover and avoided unnecessary borohydride hydrolysis.

1. INTRODUCTION

Direct borohydride fuel cells (DBFCs) have received considerable attention as alternative energy technology for applications in portable electronic devices [1-3]. However, in the case of DBFCs using an anion-exchange membrane (AEM), borohydride fuel migrates from the anode to the cathode, reducing the open-circuit potential, fuel efficiency and deactivating the cathode

catalyst [2,4]. Borohydride crossover seriously hampers the commercial viability of DBFCs. Thus, there is a continuing effort in the modification of AEM to suppress the borohydride permeability. Choudhury et al. reported that a cross-linking glutaraldehyde on a poly (vinyl alcohol) (PVA) hydrogel membrane could be used as an AEM in the DBFC [5]. The crossover rate of $NaBH_4$ was 1.8 μmol cm^{-2} h^{-1} and the utilization efficiencies of $NaBH_4$ was ~24%. An alkali-doped poly (4, 4'-diphenylether-1, 3, 4-oxadiazole) membrane was prepared and introduced into the DBFC [6]. The membrane showed comparable ion conductivity and chemical stability to Nafion® 115 in alkaline solution, but the BH_4^- permeability of the membrane (2.37 E^{-2} cm^2 min^{-1}) was higher than that of the Nafion® 115 (6.48 E^{-3} cm^2 min^{-1}). A cross-linked chitosan (CCS) membrane casted with sulfuric acid or glutaraldehyde was reported by Ma et al.[7,8]. The borohydride crossover rate through the CCS membrane casted with sulfuric acid reached 4.6×10^{-8} mol s^{-1} cm^{-2} and the coulombic efficiencies for DBFCs using the CCS membrane casted with glutaraldehyde were 33%~40%. The modification of alkali-doped PVA by CNTs not only reduced the borohydride crossover but also improved the ionic conductivity [9]. The $NaBH_4$ permeability of the PVA membrane was decreased to 3.48×10^{-3} cm^2 s^{-1} by doping CNTs. In previous work, we prepared a PVA-anion exchange resin (AER) membrane functioned by the CoOOH [10,11]. When the membrane was used in the DBFC, the fuel crossover could be inhibited through the electrocatalytic oxidation of borohydride by the CoOOH [10,11]. However, CoOOH has catalytic activity toward both borohydride oxidation and borohydride hydrolysis reactions [12,13]. Therefore, the fuel efficiency was decreased by the aggravation of the borohydride hydrolysis reaction when the membrane contacted the fuel [11].

The multilayer polymeric complexes were efficient methanol barrier agents in direct methanol fuel cells [14-17]. Jiang et al. prepared oppositely charged polyelectrolytes on a Nafion membrane

through layer-by-layer self-assembly, which could suppress the methanol crossover efficiently [14]. After cross-linking the oppositely charged amino-containing poly (ether ketone) on sulfonated poly (arylene ether ketone) bore carboxyl groups membranes to form multilayer films, the methanol permeability could be decreased to 2.99×10^{-7} cm^2 s^{-1} due to the effective block effect by the cross-linking between the anion/cation pairs [15]. The next step for the development of multilayer membranes could be the combination of both composite and multilayer concepts. That combination minimizes the disadvantages associated with highly sulfonated membranes while optimizes the advantages (such as reduced fuel crossover by composite filler membrane layer and increased proton conductivity from the sulfonated polymer) [16].

In this work, we designed a bilayer membrane, which was consisted of a PVA-AER layer and a Co-PVA-AER layer. The PVA-AER layer contacted the fuel when the membrane was assembled in the DBFC. The bilayer membrane not only improved fuel efficiency but also suppressed the borohydride crossover. The cell performance of the DBFC using the bilayer membrane was 2.14 and 1.26 times of that of the DBFC using the single PVA-AER or the single Co-PVA-AER membrane, respectively.

2. EXPERIMENTAL

The PVA-AER membrane and the Co-PVA-AER membrane were prepared as described in our previous work [10]. The bilayer membrane was made by casting the PVA-AER wet gel onto the partially desiccated Co-PVA-AER composite polymer gel. The volume ratio of the PVA-AER gel and the Co-PVA-AER get was designed to about 2:1. The thickness of the obtained bilayer membranes was about 185 μm. for comparison, the Co-PVA-AER single-layer membrane and PVA-AER single-layer membrane were similarly obtained with a thickness of about 200 μm.

X-ray diffractometer (XRD) was employed to test the crystal structure of the obtained membranes. X-ray absorption near edge structure (XANES) was used to identify the Co valence. Scanning electron microscope (SEM) and the attached energy dispersive spectrometer (EDS) were used to investigate the microstructure and chemical composition of the bilayer membrane. The spatial distribution of Co ion in the bilayer membrane was measured by X-ray fluorescence imaging at HXN of National Synchrotron Light Source-II (NSLS-II).

The swelling behaviors of membranes were conducted by measuring the swelling in thickness (SW_l) and planar (SW_a). The thicknesses and areas of wet membranes after immersion in 1 M KOH solution for 48 h and the dry membranes were measured to calculate the swelling [18]:

$$SW_l(\%) = \frac{L_{wet} - L_{dry}}{L_{dry}} \times 100 \quad (1)$$

$$SW_a(\%) = \frac{A_{wet} - A_{dry}}{A_{dry}} \times 100 \quad (2)$$

where L_{wet} and A_{wet} are the thickness and area of the wet membrane, and L_{dry} and A_{dry} are the thickness and area of the dry membrane.

The borohydride ion permeability was measured using the published method [10]. All the electrochemical tests of DBFC were performed at 30 or 60 ^{o}C respectively using a PFX-2011 battery test system (Kikusui Electronics Corp). Cell performances were tested in a single cell with an area of 2 cm×3 cm. Polypyrrole modified carbon-supported cobalt hydroxide ($Co(OH)_2$-PPy-BP) was served as both cathode catalyst and anode catalyst for single cell tests [12]. The catalyst loading was 3 mg cm^{-2}. The bilayer membrane and the single-layer membranes were utilized as the electrolyte in the cell. The fuel solution contained $NaBH_4$ (5 wt. %) and NaOH (10 wt.%), and the fuel flow rate was 10 mL min^{-1}. The oxidant was humidified O_2 with a flow rate of 100 mL min^{-1} under 0.2 MPa. The fuel efficiency test was evaluated by chronopotentiometric

curves performed under 30 °C at a constant current of 0.6 A with 20 g fuel. The durability of DBFC using the bilayer membrane was tested under 30 °C with a constant discharging current density of 50 mA cm^{-2} for 100 h.

3. RESULTS

Figure 1a shows the XRD results of the PVA-AER, bilayer and Co-PVA-AER membranes. Primary peaks at ~20 ° and minor peaks at ~40 ° are detected for all the membranes. No distinct difference is found for the XRD results of those bilayer membranes. The peaks at 20 ° and 40 ° are corresponding to the PVA matrix [10]. The XANES spectra of the bilayer membrane and the standard CoOOH sample are shown in Figure 1b. The white line peak has been pointed out by an arrow in the Figure 1(b). The position of the white line and the absorption energy of the bilayer membrane are similar to those of the standard CoOOH sample. The XRD and XANES results suggest that the Co element exists in the form of amorphous CoOOH in the bilayer membrane.

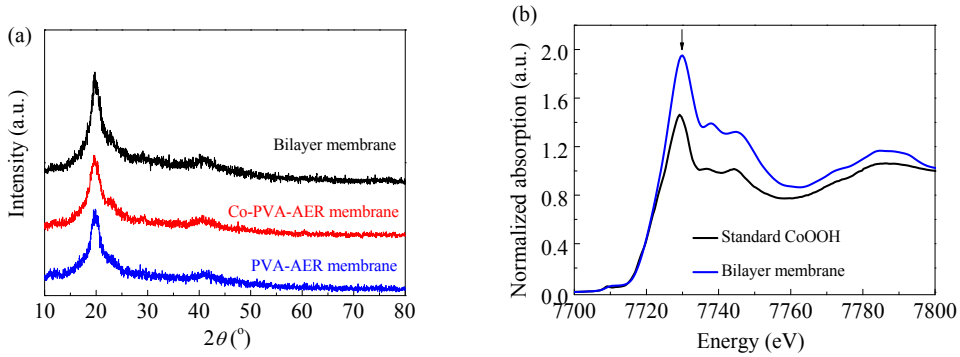

Figure 1. (a) XRD spectra of the PVA-AER, bilayer and Co-PVA-AER membranes, (b) XANES spectra of Co element in the bilayer membrane and the standard CoOOH sample.

The morphology and Co element distribution of the cross-section of the bilayer membranes are investigated by SEM and EDS (Figure 2a and 2b). The bilayer membrane has a thickness of

about 185 μm. The discontinuous distribution of Co element across the membrane clearly demonstrates the bilayer structure of the membrane (Figure 2b). The signal intensity of Co element is close to zero in the region of the PVA-AER component and notably increases to a high level in the region of the Co-PVA-AER component. The thickness of the PVA-AER component (46.5 μm) is about twice of the thickness of the Co-PVA-AER component (91.9 μm) in the bilayer membrane, which is consistent with the design ratio. The distribution of Co element in the Co-PVA-AER component is further studied by X-ray fluorescence imaging with a high spatial resolution (Figure 2c). It could been seen that the Co fluorescence signals are localized in some particles with a diameter of around 2 μm, showing an inhomogeneous distribution.

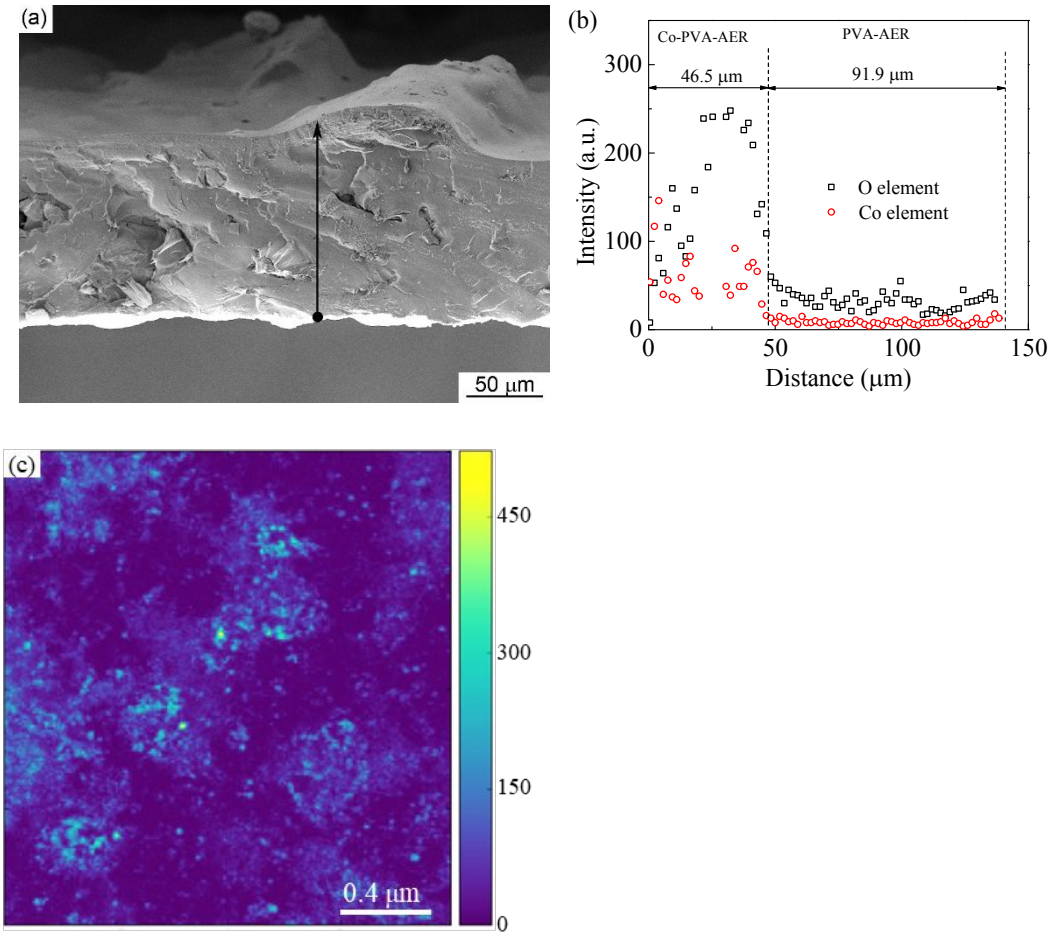

Figure 2. (a) SEM image and (b) the line scan EDS analysis on the cross-section of the bilayer membrane, (c) the distribution of Co element in the Co-PVA-AER component.

Swelling behaviors in thickness and planar dimensions of the three membranes are exhibited in Table 1. The planar swelling ratios of the Co-PVA-AER, PVA-AER, and bilayer membranes are the same as 16.7%. The thickness swelling ratios of the PVA-AER membrane and the Co-PVA-AER membrane are 15% and 12.5%, respectively. However, the thickness swelling ratio of the bilayer membrane is −10.8%. It means that the PVA-AER membrane and the Co-PVA-AER membrane thicken, but the bilayer membrane thins after immersing in alkaline solution for 48 h. The negative swelling of the bilayer membrane might be related to the interface between the Co-PVA-AER component and the PVA-AER component, which is expected to be useful in suppressing the fuel crossover.

Table 1 Swelling behavior in alkaline solution

Membranes	Planar swelling (%)	Thickness swelling (%)
Bilayer membrane	16.7	−10.8
Co-PVA-AER membrane	16.7	12.5
PVA-AER membrane	16.7	15

Figure 3 a shows the change of borohydride ion concentration (C_b) with the time. The PVA-AER membrane has the highest slope of the permeated C_b against time. The permeability is highly associated with the slope of the permeated C_b against elapsed time. The permeability is calculated according to the slope and the thickness of the membrane, as given in Figure 3b. The

permeability of the bilayer membrane is 1.34 $\times 10^{-6}$ $cm^2 \cdot s^{-1}$, which is notably lower than that of the Co-PVA-AER membrane (1.97 $\times 10^{-6}$ $cm^2 \cdot s^{-1}$) and the PVA-AER membrane (2.80 $\times$ 10^{-6} $cm^2 \cdot s^{-1}$). The suppressed fuel crossover benefits from the hydrolysis of borohydride by Co ion and the bilayer structure of the membrane.

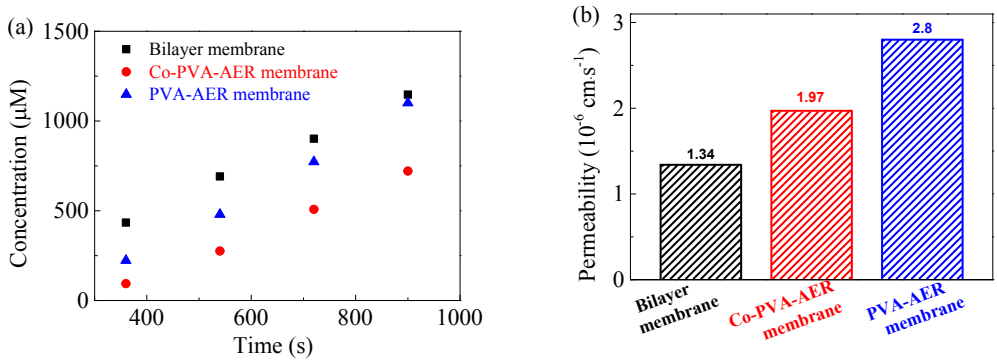

Figure 3. (a) The permeated C_b dependent on the time in the receiving compartment separated by the bilayer membrane, the Co-PVA-AER membrane and the PVA-AER membrane; (b) the permeabilities of the PVA-AER, the bilayer and the Co-PVA-AER membranes from the result of (a).

Fuel efficiency of membrane is analyzed under a constant discharge current of 0.6 A with 20 g fuel solution at 30 °C. Figure 4a shows the chronopotentiometric data of the DBFCs using the bilayer membrane, the Co-PVA-AER membrane, and the PVA-AER membrane, respectively. The final rapid drop in cell voltage is because of the fuel exhaustion. The fuel efficiency of the DBFCs using different membrane is calculated and compared in Figure 4b. The fuel efficiency of the DBFC using the bilayer membrane is higher than the others. The output power of the DBFC using the bilayer membrane is calculated to be 1.73 Wh, which is about 1.36 times that of the DBFC using the Co-PVA-AER membrane (1.27 Wh). The Co-PVA-AER membrane has lower borohydride permeability than the PVA-AER membrane. However, the fuel efficiency of

the DBFC using the Co-PVA-AER membrane is lower than that of the DBFC using the PVA-AER membrane. It was proven that the fuel crossover could be decreased by the addition of Co ion in the membrane [11]. However, the fuel efficiency of the DBFC using the Co-PVA-AER membrane is also decreased due to the aggravation borohydride hydrolysis reaction by Co ion. The bilayer structure design avoids the unexpected hydrolysis reaction by using a protective layer of the PVA-AER component. As a result, the DBFC using the bilayer membrane exhibits the highest fuel efficiency and output power.

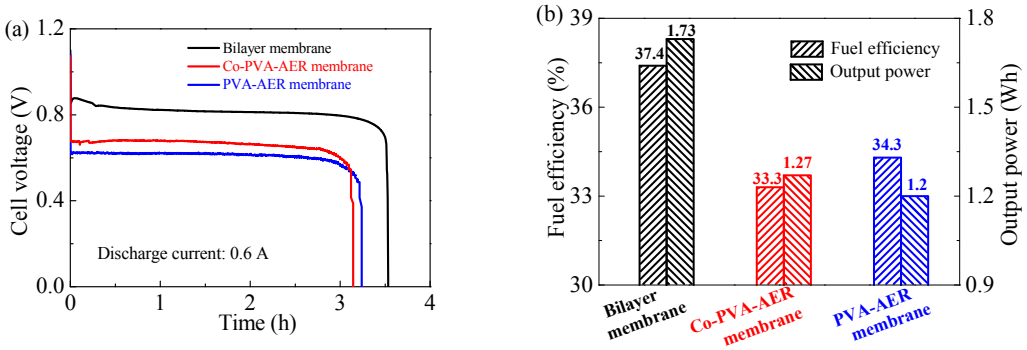

Figure 4. (a) The dependences of cell voltage with time for DBFC using the bilayer membrane, Co-PVA-AER membrane, or PVA-AER membrane. (20 g fuel: 5 wt.% $NaBH_4$-10 wt.% NaOH , discharge current: 0.6 A); (b) fuel utilization ratio and output power of the tested DBFCs.

The cell performances of the DBFCs using the bilayer membrane, the Co-PVA-AER membrane, or PVA-AER membrane are similarly tested for comparison (Figure 5). The open-circuit voltage (OCV) of the DBFC using the bilayer and the Co-PVA-AER membrane are 1.13 V and 1.11 V, which is higher than that of the DBFC using the PVA-AER membrane (1.07 V). When the operation temperature increases to 60 °C, the OCV of the DBFC using the bilayer membrane (1.086 V) is still the highest among the three sample. The higher OCV results from the suppression of fuel crossover by the Co ion in the bilayer and the Co-PVA-AER membranes. The maximum power density of 327 $mW \cdot cm^{-2}$ is achieved by the cell using the bilayer

membrane, which is notably higher than that of the cell using the Co-PVA-AER membrane (260 $mW \cdot cm^{-2}$) and the PVA-AER membrane (153 $mW \cdot cm^{-2}$) at 60 °C. The cell performance of the DBFC using the bilayer membrane is 2.14 and 1.26 times of that of the DBFC using the single PVA-AER or the single Co-PVA-AER membrane, respectively.

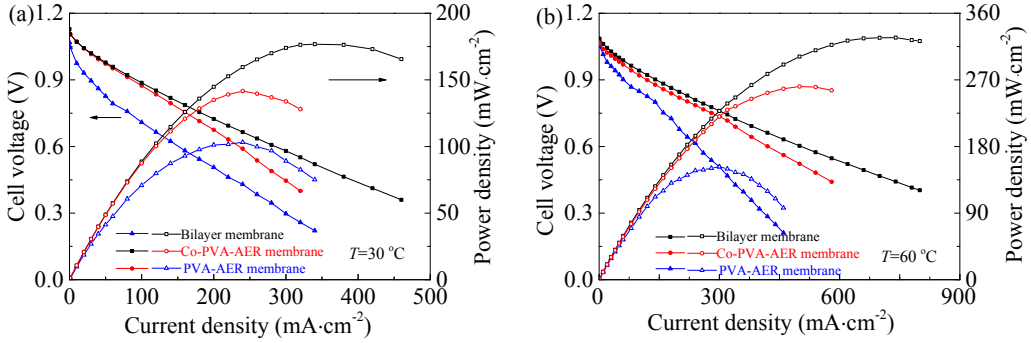

Figure 5. Performances for the cells using the bilayer membrane, the Co-PVA-AER membrane, and the PVA-AER membrane tested at (a) 30 °C and (b) 60 °C.

The stability of DBFCs using the bilayer membrane is tested at a galvanostatic discharge of 50 $mA \cdot cm^{-2}$ (Figure 6). The DBFC maintains a stable performance over100 h at 30 °C.

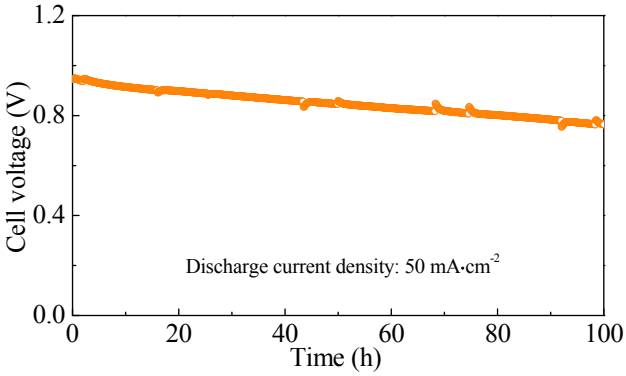

Figure 6. The stability of the DBFC using the bilayer membrane operated at 30 °C, applied current density: 50 $mA \cdot cm^{-2}$.

4. DISCUSSION

In this work, the bilayer membranes are prepared by using the layer by layer deposition method, as shown in Figure 7. The thickness of the bilayer membrane decreases from 185 to 160 μm after immersing in an alkaline solution for 48 h. Whereas the thickness of the PVA-AER membrane and the Co-PVA-AER membrane increases from 200 μm to 230 μm and 225 μm, respectively. The different change tendency of the thickness should be attributed to the interface in the bilayer membrane, which is absent in the Co-PVA-AER and the PVA-AER single-layer membrane. When a PVA-based membrane is immersed in the alkaline solution, the PVA chains absorb water molecules and therefore, the length and the interval of those PVA chains increase. As a result, the membrane expands in the thickness and on the plane. Compared to the single-layer membranes, the extra interface in the bilayer membrane restricts the expansion in the thickness direction. Considering the Poisson effect, the faster expansion on the plane and slower expansion in the thickness would lead to a slight decrease in the thickness. As a result, the bilayer membrane has a higher density of PVA chains in the thickness direction than the single-layer membranes. Yang et al. prepared a novel methanol-blocking membrane of poly(diallyldimethylammonium chloride) and graphene oxide nanosheets onto the surface of the Nafion® membrane by the layer-by-layer assembly[19]. The bilayers formed a dense film structure on the surface of the Nafion® membrane and were methanol-blocking. Therefore, the higher density of PVA chains in the thickness direction benefits for blocking the borohydride crossover, which is the main reason that the bilayer membrane possesses the lowest fuel permeability (Figure 3). Previous studies also pointed out that the fuel permeability was related to the arrangement of multilayer composite membranes [20]. Thus, the bilayer design not only avoids the unnecessary hydrolysis of borohydride to increase fuel efficiency, but also suppresses the fuel crossover to improve the cell output.

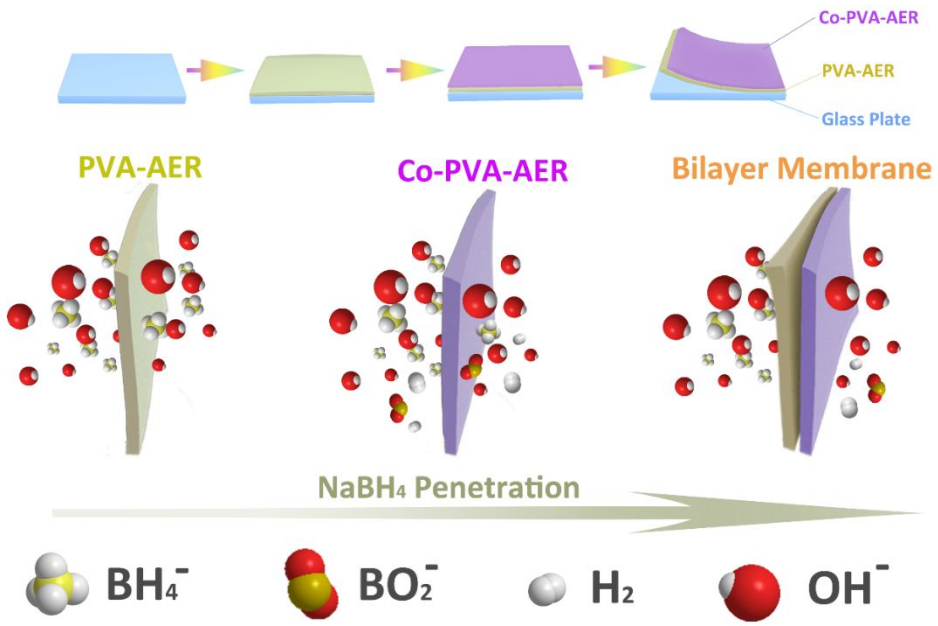

Figure 7. Schematic diagram of the bilayer membrane in this work.

5. CONCLUSION

In summary, a bilayer AEM is designed and prepared by casting a PVA-AER wet gel onto the partially desiccated Co-PVA-AER gel. The interface between the Co-PVA-AER and the PVA-AER components restricts the expansion of PVA chains in thickness direction. The bilayer membrane exhibits a negative swelling ratio in thickness. The bilayer membrane has a lower fuel permeability and higher fuel efficiency than the Co-PVA-AER and the PVA-AER single-layer membranes. The DBFCs using the bilayer membrane achieves the highest peak power density and exhibits an excellent stability over 100 h discharging at 50 $mA \cdot cm^{-2}$. Thus, the bilayer design of combining a catalytic active layer with a normal layer is a convenient and effective method to prepare high-performance membranes for fuel cells.

ASSOCIATED CONTENT

AUTHOR INFORMATION

Corresponding Author

*Haiying Qin- College of Materials and Environmental Engineering, Hangzhou Dianzi University, Hangzhou 310018, P. R. China. E-mail: hyqin@hdu.edu.cn.

Give contact information for the author(s) to whom correspondence should be addressed.

Author Contributions

The manuscript was written through contributions of all authors. All authors have given approval to the final version of the manuscript.

Funding Sources

This work is supported by the Zhejiang Provincial Natural Science Foundation of China (No. LY18B060005) and the Natural Science Foundation of Shanghai (17ZR1436800).

Notes

Any additional relevant notes should be placed here.

ACKNOWLEDGMENT

The authors appreciate HXN in National Synchrotron Light Source-II (NSLS-II). Thanks also to Dr. Gan Jia (College of Material, Chemistry and Chemical Engineering, Hangzhou Normal University) for the assistance in drawing pictures. This work is supported by the Zhejiang Provincial Natural Science Foundation of China (No. LY18B060005) and the Natural Science Foundation of Shanghai (17ZR1436800).

REFERENCES

(1) Wang, Z.; Parrondo, J.; He, C.; Sankarasubramanian, S.; Ramani, V. Efficient Ph-

Gradient-Enabled Microscale Bipolar Interfaces in Direct Borohydride Fuel Cells. *Nature Energy* **2019**, *4*, 281-289.

(2) Merino-JimÉNez, I.; Ponce De LeÓN, C.; Shah, A. A.; Walsh, F. C. Developments in Direct Borohydride Fuel Cells and Remaining Challenges. *J. Power Sources* **2012**, *219*, 339-357.

(3) Aziznia, A.; Oloman, C. W.; Gyenge, E. L. Experimental Advances and Preliminary Mathematical Modeling of the Swiss-Roll Mixed-Reactant Direct Borohydride Fuel Cell. *J. Power Sources* **2014**, *265*, 201-213.

(4) De Leon, C. P.; Walsh, F. C.; Pletcher, D.; Browning, D. J.; Lakeman, J. B. Direct Borohydride Fuel Cells. *J. Power Sources* **2006**, *155*, 172-181.

(5) N A Choudhury, S. K. P., S Pitchumani, P Sridhar and A K Shukla Poly (Vinyl Alcohol) Hydrogel Membrane as Electrolyte for Direct Borohydride Fuel Cells *J. Chem. Sci.* **2009**, *121*, 647-654.

(6) Mai, Z.; Zhang, H.; Li, X.; Geng, X.; Zhang, H. Polymer Electrolyte Based On Chemically Stable and Highly Conductive Alkali-Doped Polyoxadiazole for Direct Borohydride Fuel Cell. *Electrochem. Comm.* **2011**, *13*, 1009-1012.

(7) Ma, J.; Choudhury, N. A.; Sahai, Y.; Buchheit, R. G. A High Performance Direct Borohydride Fuel Cell Employing Cross-Linked Chitosan Membrane. *J. Power Sources* **2011**, *196*, 8257-8264.

(8) Sahai, J. M. A. Y. A Direct Borohydride Fuel Cell with Thin Film Anode and Polymer Hydrogel Membrane. *ECS Electrochem. Lett.* **2012**, *1*, 3.

(9) Huang, C.-C.; Liu, Y.-L.; Pan, W.-H.; Chang, C.-M.; Shih, C.-M.; Chu, H.-Y.; Chien, C.-H.; Juan, C.-H.; Lue, S. J. Direct Borohydride Fuel Cell Performance Using Hydroxide-Conducting Polymeric Nanocomposite Electrolytes. *J. Polymer Sci. B* **2013**, *51*, 1779-1789.

(10) Qin, H.; Lin, L.; Chu, W.; Jiang, W.; He, Y.; Shi, Q.; Deng, Y.; Ji, Z.; Liu, J.; Tao, S. Introducing Catalyst in Alkaline Membrane for Improved Performance Direct Borohydride Fuel Cells. *J. Power Sources* **2018**, *374*, 113-120.

(11) Qin, H.; Hu, Y.; Zhu, C.; Chu, W.; Sheng, H.; Dong, Z.; He, Y.; Wang, J.; Li, A.; Chi, H.; Ni, H.; Ji, Z.; Liu, J. Functionalization of Polyvinyl Alcohol Composite Membrane by Coooh for Direct Borohydride Fuel Cells. *Electrochem. Comm.* **2017**, *77*, 1-4.

(12) Qin, H. Y.; Liu, Z. X.; Ye, L. Q.; Zhu, J. K.; Li, Z. P. The Use of Polypyrrole Modified Carbon-Supported Cobalt Hydroxide as Cathode and Anode Catalysts for the Direct Borohydride Fuel Cell. *J. Power Sources* **2009**, *192*, 385-390.

(13) Wee, J. H. A Comparison of Sodium Borohydride as a Fuel for Proton Exchange Membrane Fuel Cells and for Direct Borohydride Fuel Cells. *J. Power Sources* **2006**, *155*, 329-339.

(14) Jiang, S. P.; Liu, Z.; Tian, Z. Q. Layer-By-Layer Self-Assembly of Composite Polyelectrolyte–Nafion Membranes for Direct Methanol Fuel Cells. *Adv. Mater.* **2006**, *18*, 1068-1072.

(15) Wang, J.; Zhao, C.; Lin, H.; Zhang, G.; Zhang, Y.; Ni, J.; Ma, W.; Na, H. Design of a Stable and Methanol Resistant Membrane with Cross-Linked Multilayered Polyelectrolyte Complexes for Direct Methanol Fuel Cells. *J. Power Sources* **2011**, *196*, 5432-5437.

(16) Branco, C. M.; Sharma, S.; De Camargo forte, M. M.; Steinberger-

Wilckens, R. New Approaches Towards Novel Composite and Multilayer Membranes for Intermediate Temperature-Polymer Electrolyte Fuel Cells and Direct Methanol Fuel Cells. *J. Power Sources* **2016**, *316*, 139-159.

(17) Padmavathi, R.; Karthikumar, R.; Sangeetha, D. Multilayered Sulphonated Polysulfone/Silica Composite Membranes for Fuel Cell Applications. *Electrochim. Acta* **2012**, *71*, 283-293.

(18) Yang, T.; Xu, Q.; Wang, Y.; Lu, B.; Zhang, P. Primary Study on Double-Layer Membranes for Direct Methanol Fuel Cell. *Int. J. Hydrogen Energy* **2008**, *33*, 6766-6771.

(19) Yuan, T.; Pu, L.; Huang, Q.; Zhang, H.; Li, X.; Yang, H. An Effective Methanol-Blocking Membrane Modified with Graphene Oxide Nanosheets for Passive Direct Methanol Fuel Cells. *Electrochim. Acta* **2014**, *117*, 393-397.

(20) Lue, S. J.; Pai, Y.-L.; Shih, C.-M.; Wu, M.-C.; Lai, S.-M. Novel Bilayer Well-Aligned Nafion/Graphene Oxide Composite Membranes Prepared Using Spin Coating Method for Direct Liquid Fuel Cells. *J. Membrane Sci.* **2015**, *493*, 212-223.

Table of contents

A bilayer design of combining a catalytic active layer with a normal layer is firstly proposed to realize low fuel crossover, high fuel efficiency and high power density of direct borohydride fuel cells.